The Gawler Craton Airborne Survey

Total Magnetic Intensity Grids and Magnetic Field Data Enhancements of the Merged Grids

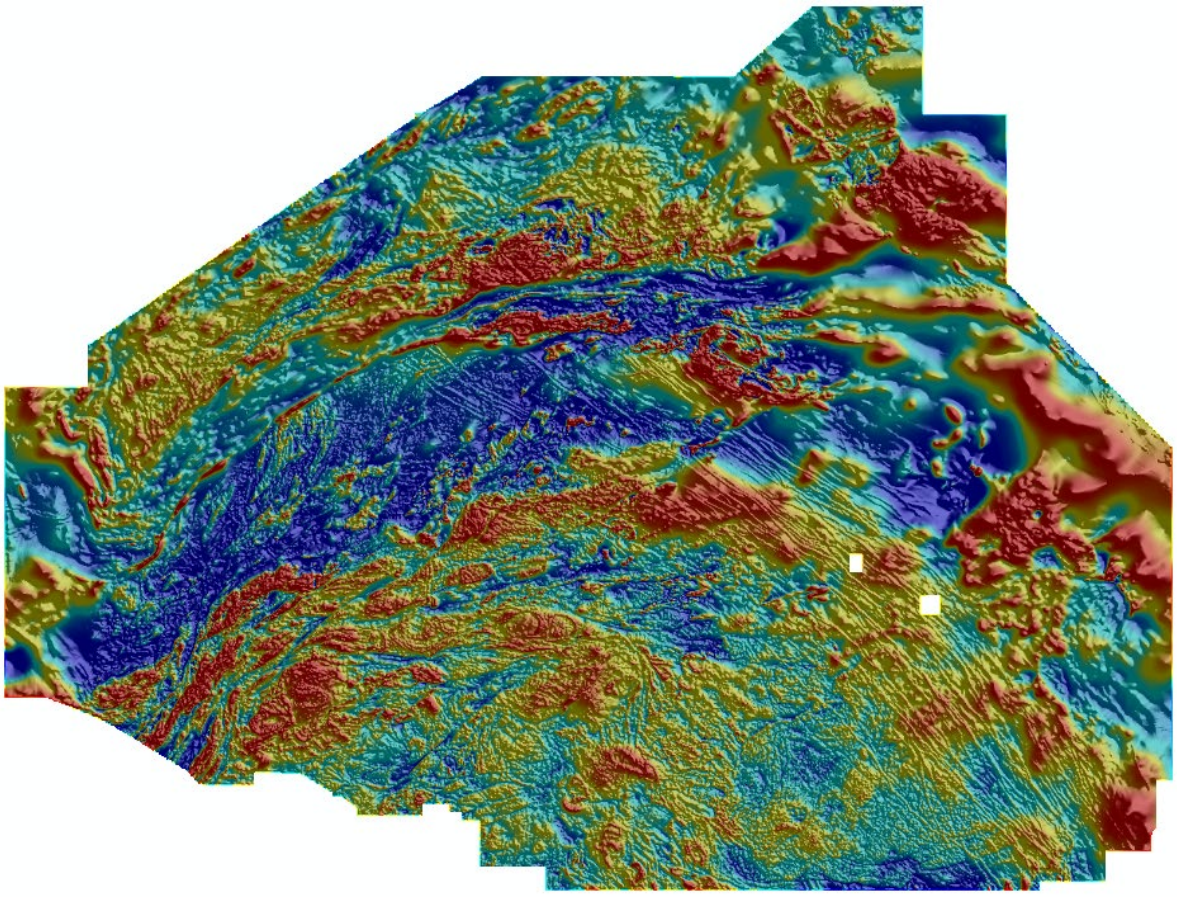

Laszlo Katona, Gary Reed, Philip Heath, George Gouthas, Jonathan Irvine

February 2021

DATA PACKAGE: GDP00117_GCAS_MERGED_TMI_GRIDS_ERS

Department for Energy and Mining
Level 4, 11 Waymouth Street, Adelaide
GPO Box 320, Adelaide SA 5001
Phone +61 8 8463 3000
Email dem.minerals@sa.gov.au
dem.petroleum@sa.gov.au
www.energymining.sa.gov.au

South Australian Resources Information Gateway (SARIG)
SARIG provides up-to-date views of mineral, petroleum and geothermal tenements and other geoscientific data. You can search, view and download information relating to minerals and mining in South Australia including tenement details, mines and mineral deposits, geological and geophysical data, publications and reports (including company reports).
map.sarig.sa.gov.au

Disclaimer
The contents of this report are for general information only and are not intended as professional advice, and the Department for Energy and Mining (and the Government of South Australia) make no representation, express or implied, as to the accuracy, reliability or completeness of the information contained in this report or as to the suitability of the information for any particular purpose. Use of or reliance upon the information contained in this report is at the sole risk of the user in all things and the Department for Energy and Mining (and the Government of South Australia) disclaim any responsibility for that use or reliance and any liability to the user.

Preferred way to cite this publication
Katona LF, Reed GD, Heath PJ, Gouthas G, Irvine JA. *The Gawler Craton Airborne Survey. Total Magnetic Intensity Grids and Magnetic Field Data Enhancements of the Merged Grids*, Data Package GDP00117_GCAS_MERGED_TMI_GRIDS_ERS. Department for Energy and Mining, South Australia, Adelaide.

Abstract:

Gawler Craton Airborne Survey (GCAS) merged magnetic (TMI), radiometric and digital elevation model (DEM) grids.

The GCAS merged datasets are the result of re-gridding and merging the sixteen GCAS TMI, Radiometric and DEM surveys' located data, using a single consistent gridding algorithm and spatial origins for each data type. In the case of the radiometric data, the located data were reprocessed by Baigent Geosciences, to retain maximum signal and achieve the highest possible degree of internal consistency in relation to data calibration and processing across the broader GCAS survey region.

The gridding was performed in the GDA94 geodetic coordinate system (which is consistent with the data capture flight lines coordinate system) at 0.00036 decimal degrees (equivalent to 40m cells). The grid origin of each of the 16 GCAS regions were carefully calculated to ensure that the resulting grids were co-nodular within the survey overlap regions to eliminate or minimise the need for resampling during processing and merging.

The gridding method used for the TMI and DEM grids was minimum curvature, for the radiometrics it was minimum curvature with tension (0.2).

TMI grids had a range of enhancements applied and are provided in the data package as ERS grids as follows:

Variable Reduction to Pole (GCAS_TMI_VRTP):

The reduction to pole (RTP) transform uses The International Geomagnetic Reference Field (IGRF) definition of the background geomagnetic field across the survey area at the time of the survey. When performing an RTP transform the IGRF at the centre of the survey region (with intensity (nT), inclination degrees and declination degrees) is used to compute the RTP. This is essentially a phase transformation of the steeply inclined geomagnetic field at the site to a vertical field (as if at the geomagnetic pole), together with a corresponding correction of the magnetisation direction from an assumed direction of the local geomagnetic field to a vertical direction (Baranov and Naudy 1964). The ideal RTP expression peaks above the source magnetisation and is only positive. Provided the assumed magnetisation direction and the specified geomagnetic field direction are both correct, the RTP image is better suited for magnetic field interpretation than the TMI image (Foss Et. al. 2020). The VRTP improves spatial precision of the RTP process by using multiple (variable) IGRF sources across the survey region instead of a single source at the centre of the region, which can cause distortions when applied to large regions.

First Vertical Derivative of the Reduced to Pole TMI (GCAS_TMI_VRTP_1VD):

Many FFT based enhancement transforms can be applied sequentially (theoretically without dependence on the sequence of operations). As decribed above, the RTP transform provides the advantage of better positioning the source magnetisations provided their magnetisation directions are as assumed. An independent advantage can be gained by calculating by FFT the vertical gradient of the magnetic field, and these two trasforms can be combined to derive the vertical gradient of the reduced-to-pole TMI. The vertical derivative of a field attenuates with distance more rapidly than does the field itself (a 1/r^4 attenuation for a magnetic dipole compared to a 1/r^3 attenuation for the field). The vertical derivative filter therefore accentuates the magnetic field expression of shallow sources. The anomalies are also sharper, providing improved lateral resolution of adjacent

sources and details of the horizontal shape of sources. The vertical derivative of the field is derived by FFT analysis through the potential field rule that the horizontal and vertical gradients form a Hilbert pair, allowing the vertical gradient to be calculated from a mapping of the horizontal gradients. The greyscale image is preferred because the absolute amplitude (well conveyed in colour) is less significant for the gradient values than for imaging of the field values, and the smoother graduations of grey tone provide a superior mapping of the sharpness of the gradients, which is controlled primarily by depth to the source magnetisation (Foss Et. al. 2020).

Second Vertical Derivative of the Reduced to Pole TMI (GCAS_TMI_VRTP_2VD):

The second vertical derivative of RTP extends the advantage of the first vertical derivative at the cost of further amplification of any short-wavelength noise. The second vertical derivative has the added characteristic that the zero contour approximately maps the edge of magnetic sources. However, this feature is of little value for regions where there are few wide sources (Foss Et. al. 2020).

Total Gradient of TMI (GCAS_TMI_AS):

The total gradient of TMI (also known as the 'analytic signal', or more correctly as the modulus of the analytic signal) is the square root of the sum of the squares of horizontal and vertical gradients. It has similar characteristics to the individual gradients in accentuating the expression of the shallowest sources and improving horizontal resolution of the fields of adjacent sources (although the use of all gradients reduces the resolution relative to images of those individual gradients). One notable characteristic of the total gradient is that it is independent of the polarity of the local change in field intensity, with low sensitivity to the influence of source magnetisation direction (Nabigian 1984; Roest et al. 1992). This transform is therefore effective in mapping the distribution of shallow magnetisations independent of their direction (Foss Et. al. 2020).

Tilt of VRTP TMI (GCAS_TMI_VRTP_TILT):

This filter is derived from the ratio of vertical and horizontal gradients transformed to an angle (range -90° to +90°) using the arc-tangent function (Miller and Singh 1994). This ratio is independent of the magnitude of the gradients and is everywhere defined, which means that it is subject to noise across regions of low gradient. The transform is effective in mapping the local trend of thin magnetic sources as well as the edges of wider magnetic sources and dislocations in this trend (Salem et al. 2008). It has slightly reduced resolution compared to the corresponding primary gradient filters (such as the first vertical derivative). With an assumption of source geometry (such as vertical edges of magnetisation distributions) depth estimates can be derived from the local widths of the tilt anomalies (for instance as measured between the -45° and +45° contours) (Foss Et. al. 2020).

Bz & Bzz (GCAS_TMI_Bz & GCAS_TMI_Bzz):

Bzz is the vertical gradient of the vertical component of the magnetic field Bz. The vertical component is derived as a phase transform of the total field (TMI) assuming that TMI is the vector in the local geomagnetic field direction. Provided this assumption is honoured, the TMI to Bz transform is independent of magnetisation direction (Lourenco and Morrison 1973). Bz provides a similar advantage to the RTP (and Bzz provides a similar advantage to the vertical gradient of RTP) without the dependence on source magnetisation direction of the RTP transform. Note that an inverted colour mapping is used in Figure 11 because in the southern hemisphere Bzz produces a negative anomaly above a normally magnetised source (Foss Et. al. 2020).

Pseudogravity (GCAS_PSEUDO_GRAVITY):

The ideal relationship between gravity and magnetic fields which would exist for an exact relationship between density and magnetisation allows the prediction of gravity field variations from magnetic field measurements (Garland 1951; Baranov 1957; Bott and Ingles 1972). This is achieved by suitable transform of the magnetic field data, namely a reduction to pole and integration known as the pseudogravity transform. Figure 16 shows the pseudogravity transform of the airborne TMI data. This image shows only partial correlation with the measured Bouguer gravity image of Figure 14 (Foss Et. al. 2020).

BigT (GCAS_TMI_GEODETIC_BigT):

BigT = sqrt(Tx* Tx + Ty* Ty + Tz* Tz)

In case of induced magnetisation only, the curvature of RTP and BigT should be in sync,if not there is the likelihood of remanence. Therefore, if the RTP tilt (curvature) is negative and the BigT tilt is positive there is remanence. This works quite well on sharp (near surface) anomalies but fails in basin areas (DFA Intrepid, 2021).

BigE (GCAS_TMI_GEODETIC_BigE):

BigE = sqrt(((Txx+ Txy+ Txz)*(Txx+ Txy+ Txz) + (Txy+ Tyy+ Tyz)*(Txy+ Tyy+ Tyz) + (Txz+ Tyz+ Txz)*(Tzz+ Txy+ Txz))/2)"

TMI TX (GCAS_TMI_GEODETIC_TX):

TX is the horizontal component (in the X direction) of the total magnetic field (TMI) derived by a phase transform (BellGeospace, 2021).

TMI TY (GCAS_TMI_GEODETIC_TY):

TY is the horizontal component (in the X direction) of the total magnetic field (TMI) derived by a phase transform.

TMI TZ (GCAS_TMI_GEODETIC_TZ):

TZ is the vertical component of the total magnetic field (TMI) derived by a phase transform.

TMI Txx (GCAS_TMI_GEODETIC_Txx):

Txx measures the rate of change of the magnetic field in the horizontal (X component).

TMI Tyy (GCAS_TMI_GEODETIC_Tyy):

Tyy measures the rate of change of the magnetic field in the horizontal (Y component).

TMI Txy (GCAS_TMI_GEODETIC_Txy):

Txy measures the rate of change of the magnetic field in the horizontal (XY component).

TMI Txz (GCAS_TMI_GEODETIC_Txz):

Txz measures the horintal rate of change in the downward direction of the horizontal components (Txx and Txy).

TMI Tyz (GCAS_TMI_GEODETIC_Tyz):

Tyz measures the horintal rate of change in the downward direction of the horizontal components (Tyy and Tyx).

TMI Tzz (GCAS_TMI_GEODETIC_Tzz):

Combination of Txx and Tyy provide a measurement in the downward component (Tzz - vertical gradient).

TMI Vecto Residual Magnetic Intensity (GCAS_TMI_GEODETIC_VRMI):

The VRMI "Vecto Residual Magnetic Intensity" filter aims to calculate the magnitude of the vector difference between the TMI and the inducing field.

Automatic Gain Control of the VRTP TMI (GCAS_TMI_VRTP_AGC):

The Automatic Gain control filter (AGC) converts magnetic waveforms of variable amplitude into waveforms of close to constant amplitude. This removes amplitude characteristics from the grid file and results in a grid that equalises the high and low amplitudes (Milligan & Gunn, 1997).

Acknowledgements

The GSSA gratefully acknowledges all who have contributed to the success of the GCAS project including:

Ursula Michael (GSSA), Geoscience Australia - in particular Matthew Hutchens and David McInnes; Baigent Geosciences; Minty Geophysics; MagSpec Airborne Surveys Pty Ltd; Sander Geophysics, Thomson Aviation Airborne Geophysical Survey; GPX Surveys

References:

Baranov V 1957. A new method for interpretation of aeromagnetic maps: pseudo-gravimetric anomalies. *Geophysics* 22:359–383.

Bott MHP and Ingles A 1972. Matrix methods for joint interpretation of two-dimensional gravity and magnetic anomalies with application to the Iceland-Faeroe Ridge. *Geophysical Journal of the Royal Astronomical Society* 30: 55–67.

DFA INTREPID V6.1.4 2021. Sample_Data, Cookbook, magnetics, remanence, REM_2_Tasks,4.3 GCAS Components.

Foss CA, Gouthas G, Wise T, Katona LF, Hutchens MF, Reed GD and Heath PJ 2020. *Gawler Craton Airborne Geophysical Survey Region 9B, Kingoonya – Enhanced geophysical imagery and magnetic source depth models*, Report Book 2020/00018. Department for Energy and Mining, South Australia, Adelaide.

Garland GD 1951. Combined analysis of gravity and magnetic anomalies. *Geophysics* 16:51–62.

Lourenco JS and Morrison HF 1973. Vector magnetic anomalies derived from measurements of a single component of the field. *Geophysics* 38:359–368.

Miller HG and Singh VJ 1994. Potential field tilt – a new concept for location of potential field sources. *Applied Geophysics* 32:213–217.

Milligan PR and Gunn PJ, 1997. Enhancement and presentation of airborne geophysical data. AGSO Journal of Australian Geology & Geophysics. 17(2), 63-75

Nabigian MN 1984. Towards a three-dimensional automatic interpretation of potential field data. *Geophysics* 49:780–786.

Online: BELLGeospace website (bellgeo.com/what-is-ftg), accessed February, 2021.

Roest WR, Verhoef J and Pilkington M 1992. Magnetic interpretation using the 3-D analytic signal. *Geophysics* 57:116–125.

Salem A, Williams S, Fairhead D, Smith R and Ravat D 2008. Interpretation of magnetic data using tilt-angle derivatives. *Geophysics* 73: L1–L10.